Bayesian Inversion of Finite Fault Models Using Open Ocean Tsunami Waveforms for the 2007 M_w 8 Pisco, Peru Earthquake

Junle Jiang, Anthony Sladen, Sarah Minson, Mark Simons
Geophysics, Division of Geological & Planetary Sciences, Caltech

Introduction

Conventional inverse problems are tackled with optimization approaches. With regularization, a single "best" model is produced for the often under-determined inverse problem. In contrast, Bayesian approach produces a posterior distribution of models through sampling, and it has its advantages over optimization that it explores the whole solution space, reveals uncertainties in the models, and involves no regularization where trade-off is imposed between model-variance and misfit.

We apply Bayesian sampling to the inverse problem of finite fault models for the 2007 M_w 8.0 Pisco, Peru earthquake. Tsunami waveforms were recorded in 5 open ocean tsunameters for this megathrust earthquake. The inversion of tsunami waveforms is expected to provide more constraint on the up-dip slip distribution on the fault, in addition to previous study (Sladen et al, JGR, 2010)

Bayesian Approach to Inverse Problem

Bayesian Sampling

A probabilistic approach that samples models in the solution space proportionally to how consistent the models are with data (likelihood), given certain prediction error, as well as with our presumption (prior information), producing a distribution of possible models (posterior) for the inverse problem.

Sampling Criteria: Bayes' Theorem

$$P(\theta \mid D) \propto P(D \mid \theta) P(\theta)$$

Model θ Data D

Posterior distribution — Likelihood — Prior distribution

$$\exp\left[-\frac{1}{2}(\mathbf{d}-\mathbf{Gm})^{T}\mathbf{C}_{\mathbf{d}}^{-1}(\mathbf{d}-\mathbf{Gm})\right]$$

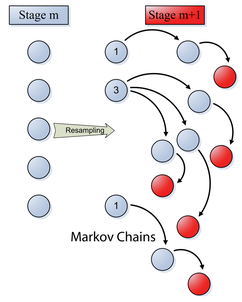

Fig. 1 Sampling procedures of CATMIP (Cascading Adaptive Tempered Metropolis in Parallel, Minson, 2010) during one cooling step (See Sarah Minson's Poster for detail)

2007 M_w 8 Pisco, Peru Earthquake

Open Ocean Tsunami Waveforms

Recorded on 5 seafloor bottom pressure recorders, established mostly in 2007 as part of DART (Deep-Ocean Assessment and Reporting of Tsunamics) buoy system in the Pacific Ocean (Fig. 3)

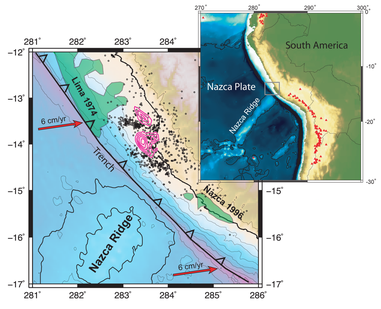

Fig. 2 Tectonic Setting

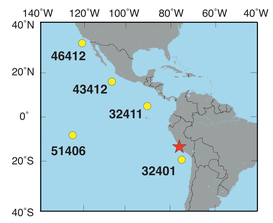

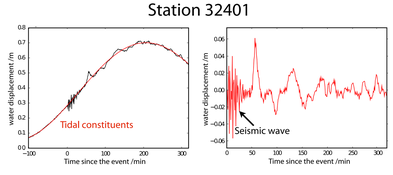

Fig. 3 Locations of tsunameters and hypocenter (top); tsunami waveforms before and after removal of tidal constituents

Inversion for Synthetic Models

Tsunami Model

COMCOT (Cornell Multi-gridded Coupled Tsunami Model)
(i) Seafloor deformation (Okada, 1985); (ii) Shallow water wave propagation.

Synthetic Fault Plane

2-D flat fault plane defined by the location of trench and hypocenter (Fig. 4)

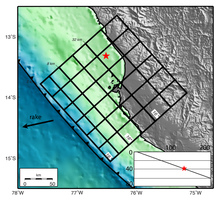

Fig. 4 2D fault plane for synthetic data
Strike: 318° Dip: 16° Rake: 63°

Prior Information
$U_{\parallel} \in$ uniform [Umin, ∞];
$U_{\perp} \in$ normal [0, σ], σ~0.5 m
initial $U_{\parallel}$ constrained by M_w

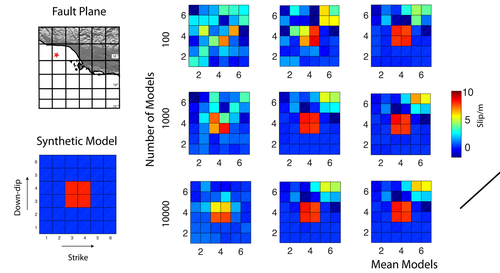

Fig. 5 Inversion results for synthetic models with different lengths of Markov chains and numbers of sampling models (prediction error: 1cm)

Model Resolution

Tsunami waveforms constrain up-dip slip well, and yet down-dip slip poorly, as is clearly shown in the posterior distributions of sampled models (Fig. 5 & 6)

Kullback-Leibler Information Divergence

Distances of the posterior distributions from a uniform distribution, also a measure of information gain during the sampling process (1 corresponds to perfect peak)

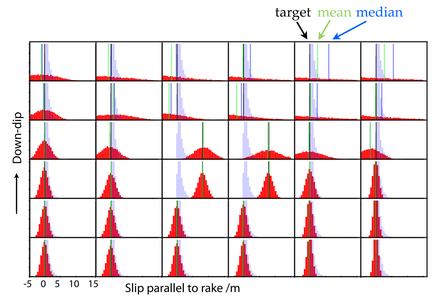

Fig. 6 Initial distribution (blue) and posterior distribution of parallel-rake slip on each patch of the fault plane. Target values of the synthetic model, mean and median values of posterior distributions are marked as black, green, and blue lines

$$D_{KL}(P \parallel Q) = \sum_i P(i) \log \frac{P(i)}{Q(i)}$$

$$\forall P(i) > 0 : Q(i) > 0 \qquad \sum_i P(i) = 1, \sum_i Q(i) = 1.$$

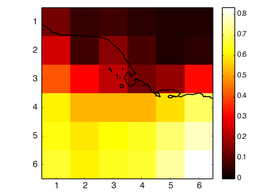

Fig. 7 KLID for the posterior distributions on the left, marked with the approximate location of shoreline

Comparison: Inversion of Synthetic InSAR data for the same model

InSAR data constrain down-dip slip much better with all 6 synthetic interferograms (5 times more data than tsunami records), still unable to well constrain offshore part of the fault

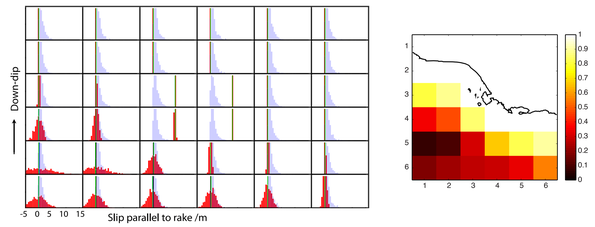

Joint Inversion

Tsunami waveforms provide complementary constraint on slip on the off-shore part of the fault

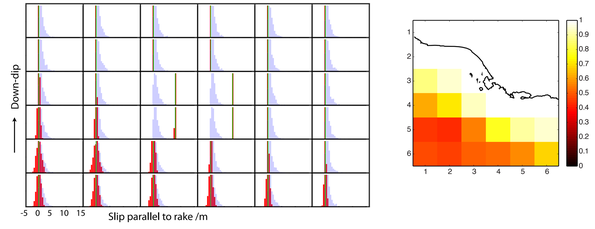

Inversion of Real Waveforms

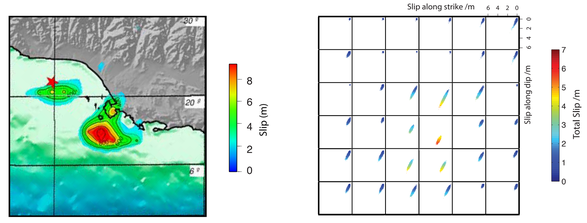

Fig. 8 Joint inversion results of InSAR and teleseismic data using optimization approach (left, Sladen et al, JGR, 2010); Inversion results of tsunami waveforms using Bayesian approach (right), every model of the posterior distribution is plotted as one point on each patch.

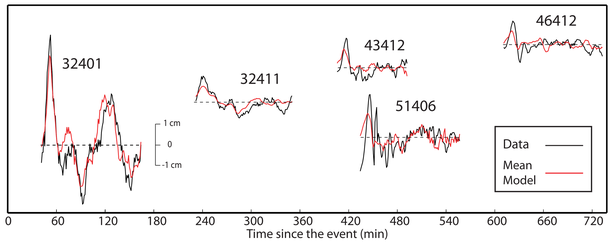

Fig. 9 Data and predicted waveforms from the mean values of the posterior distribution for the 5 tsunameters. Arrival times of tsunami waveforms are also shown

Conclusions and Future work

Conclusions: (1) Open ocean tsunami waveforms that are initiated by a megathrust earthquake can be used to rapidly invert for the static slip on the fault. (2) By means of Bayesian sampling, we can obtain a posterior distribution of finite fault models for the 2007 Mw 8 Pisco, Peru earthquake, providing us with a probabilistic description of earthquake source characteristics. (3) By the measure of KLID, we can see the intrinsic model resolution for tsunami waveforms, which, contrary to InSAR data, constrains up-dip slip better than down-dip slip on the fault.

Future work: (1) Incorporation of real InSAR data; (2) Inversion for kinematic models; (3) further posterior analysis

Acknowledgement to Gordon and Betty Moore Foundation